DMD Fast Forward. Published on March 2, 2017 as DOI: 10.1124/dmd.116.074179
This article has not been copyedited and formatted. The final version may differ from this version.

Assessing the risk of drug-induced cholestasis using unbound intrahepatic concentrations

Julia Riede, Birk Poller, Jörg Huwyler, Gian Camenisch

Division of Drug Metabolism and Pharmacokinetics, Integrated Drug Disposition Section, Novartis Institutes for BioMedical Research, CH-4056 Basel, Switzerland (JR, BP, GC)

Department of Pharmaceutical Sciences, Division of Pharmaceutical Technology, University of Basel, CH-4056 Basel, Switzerland (JR, JH)

Running Title

Unbound intrahepatic drug concentrations predict cholestasis

Corresponding author

Gian Camenisch

Novartis Pharma AG

Fabrikstr.14

CH-4056 Basel

Email: gian.camenisch@novartis.com

Mobile: +41 79 278 58

Fax: +41 61 696 85 83

Number of text pages: 30

Number of tables: 2

Number of figures: 7

Number of references: 56

Number of words in abstract: 250

Number of words in introduction: 697

Number of words in discussion: 1649

DMD Fast Forward. Published on March 2, 2017 as DOI: 10.1124/dmd.116.074179
This article has not been copyedited and formatted. The final version may differ from this version.

List of abbreviations

ALT	alanine aminotransferase
AP	alkaline phosphatase
BSEP	bile salt export pump
$C_{hep,inlet,max,u}$	unbound intrahepatic concentration on basis of $C_{inlet,max,u}$
$C_{hep,inlet,u}$	unbound intrahepatic concentration on basis of $C_{inlet,u}$
$C_{hep,sys,u}$	unbound intrahepatic concentration on basis of $C_{sys,u}$
$C_{hep,u}$	unbound intrahepatic concentration
$C_{inlet,max,u}$	"worst-case assessment" of unbound concentration at the hepatic inlet
$C_{inlet,u}$	unbound concentration at the hepatic inlet
C_{max}	maximum plasma concentration
$C_{sys,u}$	unbound systemic concentration
C_u	unbound extracellular concentration
CL_{int}	intrinsic clearance
$CL_{int,h}$	intrinsic hepatic clearance
$CL_{int,met}$	intrinsic metabolic clearance
$CL_{int,sec}$	intrinsic biliary clearance
CYP	cytochrome P450
DDI	drug-drug interactions
DIC	drug-induced cholestasis
DILI	drug-induced liver injury
ECM	Extended Clearance Model
IC_{50}	half maximal inhibitory concentration
IVIVC	*in vitro-in vivo* correlation
IVIVE	*in vitro-in vivo* extrapolation
Kp_{uu}	liver-to-blood partition coefficient for unbound drug at steady-state
MRP	multidrug resistance protein
NADPH	nicotinamide adenine dinucleotide phosphate

DMD Fast Forward. Published on March 2, 2017 as DOI: 10.1124/dmd.116.074179
This article has not been copyedited and formatted. The final version may differ from this version.

OATP	organic anion transporting polypeptide
PAH	pulmonary arterial hypertension
PS_{eff}	sinusoidal efflux clearance
$PS_{eff,act}$	active sinusoidal efflux clearance
$PS_{eff,pas}$	passive sinusoidal efflux clearance
PS_{inf}	total sinusoidal uptake clearance
$PS_{inf,act}$	active sinusoidal uptake clearance
$PS_{inf,pas}$	passive sinusoidal uptake clearance
ROC AUC	area under the receiver operating characteristic curve
UDP	uridine diphosphate
UGT	UDP-glucuronosyltransferase
ULN	upper limit of normal

DMD Fast Forward. Published on March 2, 2017 as DOI: 10.1124/dmd.116.074179
This article has not been copyedited and formatted. The final version may differ from this version.

Abstract

Inhibition of the bile salt export pump (BSEP) has been recognized as a key factor in the development of drug-induced cholestasis (DIC). The risk of DIC in human has previously been assessed using *in vitro* BSEP inhibition data (IC_{50}) and unbound systemic drug exposure under assumption of the "free drug hypothesis". This concept, however, is unlikely valid as unbound intrahepatic drug concentrations are affected by active transport and metabolism. To investigate this hypothesis we experimentally determined the *in vitro* liver-to-blood partition coefficients (Kp_{uu}) for 18 drug compounds using the hepatic Extended Clearance Model (ECM). *In vitro-in vivo* translatability of Kp_{uu} values was verified for a subset of compounds in rat. Consequently, unbound intrahepatic concentrations were calculated from clinical exposure (systemic and hepatic inlet) and measured Kp_{uu} data. Using these values, corresponding safety margins against BSEP IC_{50} values were determined and compared to the clinical incidence of DIC. Depending on the ECM class of a drug, *in vitro* Kp_{uu} values deviated up to 14-fold from unity and unbound intrahepatic concentrations were affected accordingly. The use of *in vitro* Kp_{uu}-based safety margins allowed to separate clinical cholestasis frequency into three classes (no cholestasis, cholestasis in ≤ 2%, and in > 2% of subjects) for 17 out of 18 compounds. This assessment was significantly superior compared to using unbound extracellular concentrations as a surrogate for intrahepatic concentrations. Furthermore, the assessment of Kp_{uu} according to ECM provides useful guidance for the quantitative evaluation of genetic and physiological risk factors for the development of cholestasis.

DMD Fast Forward. Published on March 2, 2017 as DOI: 10.1124/dmd.116.074179
This article has not been copyedited and formatted. The final version may differ from this version.

Introduction

The liver is the major organ involved in the elimination of potentially harmful endogenous and xenobiotic substances, including pharmaceutical drugs, and is itself predisposed to toxicity resulting from high exposure to drugs and their metabolites. Drug-induced liver injury (DILI) is a leading cause for acute liver failure, termination of compounds in drug development and drug withdrawal from the market (Lee, 2003; FDA, 2009). The severity of DILI ranges from asymptomatic elevations of liver enzymes to acute liver failure and manifests with hepatocellular, cholestatic or mixed (hepatocellular/cholestatic) patterns.

Although drug-induced cholestasis (DIC) usually represents a less severe form of DILI, it is nevertheless reported to account for up to 26% of all hepatic adverse reactions (Bjornsson and Olsson, 2005; Hussaini and Farrington, 2007). Cholestasis is characterized by reduced bile flow, potentially resulting in accumulation of cytotoxic bile salts within hepatocytes leading to liver damage (Stieger, 2010). The bile salt export pump (BSEP), a member of the ATP-binding cassette superfamily encoded by the ABCB11 gene, is expressed at the canalicular membrane of hepatocytes and plays a fundamental role in bile homeostasis by secreting bile acids from the hepatocyte into bile ducts. Impairment of BSEP function due to inhibition by drugs or genetic defects was previously identified as a key factor in the development of DIC, hereditary cholestatic syndromes or intrahepatic cholestasis of pregnancy (Stieger et al., 2000; Fattinger et al., 2001; Funk et al., 2001; Pauli-Magnus et al., 2010; Dietrich and Geier, 2014). Several attempts have been made to predict DIC or DILI in humans from *in vitro* BSEP inhibition data due to limited translatability of hepatic adverse events from preclinical models (Olson et al., 2000). Recently, Dawson et al. (2012) and Morgan et al. (2013) demonstrated that potent BSEP *in vitro* inhibition and high systemic drug exposure correlates with the occurrence of DIC. However, the assessments did not allow clearly separating cholestatic/mixed from non-cholestatic drugs, and thus reliable prediction of DIC remains challenging.

Clinical drug toxicity, drug-drug interactions (DDI) and pharmacological drug-target interactions are commonly anticipated by relating the *in vitro* target potency (IC_{50}, K_i or EC_{50}

value) to the unbound (i.e. free) systemic drug concentration due to limited availability of tissue concentration data in humans (Muller and Milton, 2012; Zamek-Gliszczynski et al., 2013). This assessment is based on the ”free drug hypothesis“, which assumes complete distribution equilibrium of the unbound drug between blood and tissue at steady-state. This assumption, however, is unlikely to apply for organs such as the liver, where the distribution equilibrium is affected by active cellular transport and metabolic processes (Chu et al., 2013). Therefore, recent publications proposed to estimate the unbound intracellular liver concentration using the liver-to-blood partition coefficient for unbound drug at steady-state (Kp_{uu}) *in vitro* (Yabe et al., 2011; Mateus et al., 2013; Pfeifer et al., 2013; Shitara et al., 2013; Nicolai et al., 2015). Following the concept of the hepatic Extended Clearance Model (ECM), the *in vitro* (hepatocyte-to-medium) Kp_{uu} can be derived from *in vitro* measurements of individual hepatic elimination process clearances (sinusoidal influx and efflux, metabolism and biliary secretion), which govern hepatic elimination (Fig. 1) (Shitara et al., 2013; Camenisch et al., 2015; Camenisch, 2016). Measurements of individual hepatic process clearances additionally allow assignment of compounds into four distinct ECM categories to anticipate class-dependent effects on Kp_{uu} and, as a consequence, on the unbound intracellular concentration (Fig. 2) (Camenisch et al., 2015; Camenisch, 2016).

The aim of the present study was to identify the reference drug concentration (unbound systemic, unbound hepatic inlet or unbound intrahepatic concentration) that provides the best anticipation of DIC risk due to BSEP inhibition. Upon assessing *in vitro-in vivo* correlation (IVIVC) for Kp_{uu} in rat using literature data, we experimentally determined human hepatic *in vitro* Kp_{uu} values using the ECM concept for 18 drug compounds with diverse physicochemical and pharmacokinetic properties. Unbound intrahepatic concentrations in human were estimated by applying ECM-based Kp_{uu} to either unbound systemic or hepatic inlet concentrations. The resulting safety margins between *in vitro* BSEP IC_{50} and the various reference concentrations were compared to the clinical incidence of DIC. In addition, the potential impact of genetic and physiological risk factors on the induction of cholestasis is discussed using bosentan as tool compound.

DMD Fast Forward. Published on March 2, 2017 as DOI: 10.1124/dmd.116.074179
This article has not been copyedited and formatted. The final version may differ from this version.

Materials and Methods

Materials. Radiolabeled test compounds ([^{3}H] or [^{14}C]) were obtained from PerkinElmer (Boston, MA), American Radiolabeled Chemicals (St. Louis, MO) and Moravek Biochemicals (Brea, CA). Radiochemical purity of all compounds was ≥95% as determined in-house by HPLC analysis. All other chemicals were purchased from commercial sources and were of analytical grade.

Determination of hepatic *in vitro* Kp_{uu}. Previous work performed by our group has shown that *in vivo* hepatic organ clearances (CL_h) were correctly predicted by feeding up-scaled *in vitro* hepatic process clearances into the ECM (eq. 1) and by applying the "well-stirred" liver model (eq. 2) (Camenisch and Umehara, 2012; Umehara and Camenisch, 2012; Kunze et al., 2015):

$$CL_{h,int} = \frac{PS_{inf,act}+PS_{inf,pas}}{PS_{eff,act}+PS_{eff,pas}+CL_{int,met}+CL_{int,sec}} \times (CL_{int,met} + CL_{int,sec})$$

$$= \frac{PS_{inf}}{PS_{eff}+CL_{int}} \times CL_{int} \quad (1)$$

$$CL_h = \frac{Q_h \times fu_b \times CL_{h,int}}{Q_h + fu_b \times CL_{h,int}} \quad (2)$$

where $CL_{h,int}$ is the intrinsic hepatic clearance, PS_{inf} is the sum of active ($PS_{inf,act}$) and passive uptake membrane permeability ($PS_{inf,pas}$), PS_{eff} is the sum of active ($PS_{eff,act}$) and passive sinusoidal efflux membrane permeability ($PS_{eff,pas}$), CL_{int} is the sum of intrinsic metabolic ($CL_{int,met}$) and biliary clearances ($CL_{int,sec}$), Q_h is the hepatic blood flow and fu_b is the unbound fraction in blood.

This *in vitro-in vivo* extrapolation (IVIVE) approach for human and rat hepatic clearance provided a good prediction accuracy for a diverse dataset of 13 compounds with ~80% within two-fold error (Camenisch and Umehara, 2012; Umehara and Camenisch, 2012). According to the concept of the ECM, the intrinsic clearance is driven by the intracellular concentration (Shitara et al., 2013) and eq. 1 can be rearranged as follows:

$$CL_{h,int} = Kp_{uu} \times CL_{int} \quad (3)$$

Hepatic process clearances. Hepatic process clearances for 18 test compounds were experimentally determined as previously described in full detail elsewhere (Camenisch and

DMD Fast Forward. Published on March 2, 2017 as DOI: 10.1124/dmd.116.074179
This article has not been copyedited and formatted. The final version may differ from this version.

Umehara, 2012; Umehara and Camenisch, 2012; Kunze et al., 2014; Kunze et al., 2015). All presented *in vitro* data for atorvastatin, cerivastatin, cyclosporine A, fluvastatin, ketoconazole, lovastatin acid, pitavastatin, pravastatin, rosuvastatin, simvastatin acid and verapamil were taken from Camenisch and Umehara (2012) and Kunze et al. (2015).

Briefly, $PS_{inf,act}$ and $PS_{inf,pas}$ were determined in pooled suspended human hepatocytes using the oil-spin method. $PS_{inf,act}$ and $PS_{inf,pas}$ represent single time point measurements within the linear time and concentration range, $PS_{inf,pas}$ was determined in the presence of uptake transporter inhibitors or at high substrate concentrations where active transport processes are known to be saturated. Measured (apparent) uptake clearances were corrected for non-specific binding to the assay device using radioactivity recoveries and for saturable binding to cell surfaces using data from control incubations at 4°C (Kunze et al., 2014). For the highly lipophilic compounds ketoconazole and atazanvir ($logD_{7.4} > 4$) PS_{inf} was determined from the slope of initial uptake velocity (3 time points between 0.5 - 3 min) taking into account initial cellular binding and non-specific binding to the assay device.

PS_{eff} was assumed to occur only via passive diffusion and to be equal to $PS_{inf,pas}$ ($PS_{eff,act} = 0$, $PS_{eff,pas} = PS_{inf,pas}$).

Apparent metabolic clearance ($CL_{int,met,app}$) was determined using human liver microsomes. Incubations with all test compounds were performed in the presence of nicotinamide adenine dinucleotide phosphate (NADPH). The known uridine diphosphate (UDP)-glucuronosyltransferase (UGT) substrates cerivastatin, fluvastatin, ibuprofen, pitavastatin and simvastatin acid were additionally incubated in the presence of UDP and $CL_{int,met}$ represents the sum of NADPH and UDP incubations. $CL_{int,met,app}$ values were corrected for the unbound fraction in liver microsomes (fu_{mic}) as follows:

$$CL_{int,met} = \frac{CL_{int,met,app}}{fu_{mic}} \quad (4)$$

Values for fu_{mic} and corresponding literature references are provided in Supplemental Table 4.

DMD Fast Forward. Published on March 2, 2017 as DOI: 10.1124/dmd.116.074179
This article has not been copyedited and formatted. The final version may differ from this version.

Apparent biliary clearance ($CL_{int,sec,app}$) was determined in sandwich-cultured human hepatocytes (B-CLEAR® method, Qualyst, Inc., Durham, NC) and was corrected for the unbound fraction in hepatocytes (fu_{hep}) as given in eq. 5:

$$CL_{int,sec} = \frac{CL_{int,sec,app}}{fu_{hep}} \quad (5)$$

fu_{hep} values were derived from $logD_{7.4}$ as follows (Yabe et al., 2011):

$$log(fu_{hep}) = -0.9161 - 0.2567 \times logD_{7.4} \quad (6)$$

Values for $logD_{7.4}$ and corresponding literature references are provided in Supplemental Table 4.

The *in vitro* clearances were up-scaled to human organ level [ml/min/kg] using the following scaling factors: 99 [10^6 cells/g liver] for suspended hepatocytes, 53 [mg protein/g liver] for HLM, 116 [mg protein/g liver] for sandwich-cultured hepatocytes and 25.7 [g liver/kg body weight] for liver weight.

Calculation of unbound drug concentrations in the systemic circulation, at the hepatic inlet and in the hepatocyte. Unbound drug concentrations in blood and plasma are equal (Kwon, 2001) and herein referred to as unbound systemic drug concentrations ($C_{sys,u}$). $C_{sys,u}$ was calculated from the total maximum available drug plasma concentration (C_{max}) at steady-state upon oral administration of the maximum recommended dose in healthy human subjects and the fraction unbound in plasma (fu_p):

$$C_{sys,u} = C_{max} \times fu_p \quad (7)$$

Unbound drug concentrations at the hepatic inlet ($C_{inlet,u}$) were calculated according to eq. 8 as the sum of drug in the systemic circulation reaching the liver via the hepatic artery (i.e. $C_{sys,u}$) and drug that is delivered by the portal vein upon intestinal absorption (Giacomini et al., 2010):

$$C_{inlet,u} = C_{sys,u} + \frac{fu_p \times k_a \times F_a \times F_g \times D}{Q_h \times R_b} \quad (8)$$

where k_a is the absorption rate constant, F_a is the fraction absorbed, F_g is the fraction escaping gut metabolism, D is the maximum recommended single oral dose, Q_h is the hepatic blood flow (1.45 l/min) and R_b is the blood-to-plasma partition coefficient.

DMD Fast Forward. Published on March 2, 2017 as DOI: 10.1124/dmd.116.074179
This article has not been copyedited and formatted. The final version may differ from this version.

Additionally, maximum unbound hepatic inlet concentrations ($C_{inlet,max,u}$), representing a "worst-case", were calculated according to eq. 8 assuming complete and fast drug absorption (i.e. $F_a \times F_g = 1$ and $k_a = 0.1\ min^{-1}$) (Ito et al., 1998).

Unbound intracellular drug concentrations in the hepatocyte (hereafter referred as unbound intrahepatic concentration ($C_{hep,u}$)) were either calculated on basis of $C_{sys,u}$ (eq. 9), $C_{inlet,u}$ (eq. 10) or $C_{inlet,max,u}$ (eq. 11):

$$C_{hep,sys,u} = Kp_{uu} \times C_{sys,u} \quad (9)$$

$$C_{hep,inlet,u} = Kp_{uu} \times C_{inlet,u} \quad (10)$$

$$C_{hep,inlet,max,u} = Kp_{uu} \times C_{inlet,max,u} \quad (11)$$

All clinical exposure data, pharmacokinetic parameters and calculations thereof are provided in the supplemental material together with the corresponding literature references (Supplemental Tables 2 – 4).

Human BSEP IC_{50} values. *In vitro* IC_{50} data for BSEP inhibition were collected from the literature. In case of multiple reported values the lowest one was used for risk assessments (Table 1), while Supplementary Table 5 shows the range of reported data. All data have been determined under comparable conditions using membrane vesicles expressing human BSEP with [^{3}H]taurocholate as probe substrate.

Cholestasis classification. Cholestasis annotation was carried out exclusively on the basis of clinical studies, drug labels and comprehensive literature search where cholestasis or mixed liver injury was observed under controlled conditions (i.e. declaration of co-medication, underlying disease state, known dosing regimen). Drugs were categorized as "cholestatic" based on reports of one of the following adverse events: cholestasis, cholestatic liver injury, cholestatic jaundice, cholestatic hepatitis, mixed liver injury, or biochemical evidence of cholestasis or mixed liver injury in form of elevated serum alkaline phosphatase (AP) (AP ≥ 2x upper limit of normal (ULN) and ratio between alanine aminotransferase (ALT) ULN and AP ULN < 5) (CIOMS, 1999). Based on the reported cholestasis incidence drugs were assigned into the sub-classes "common" (> 2% of subjects) or "rare" (≤ 2% of subjects). In the absence of above defined cholestasis events, drugs were categorized as "no

DMD Fast Forward. Published on March 2, 2017 as DOI: 10.1124/dmd.116.074179
This article has not been copyedited and formatted. The final version may differ from this version.

cholestasis". The threshold of 2% was selected based on literature information from clinical reports or from the drug label, where rare adverse events were commonly defined as < 2%. Detailed cholestasis annotations and literature references are summarized in Supplemental Table 5.

Data analysis. The DIC risk was assessed based on safety margins, calculated as the ratio between BSEP IC_{50} and the unbound intrahepatic drug concentration. Following the static R-value approach for reversible enzyme or transporter inhibition and using $C_{max,u}$ as basis for unbound intrahepatic concentrations the assessment represents a "worst-case" scenario for DIC (Rowland and Matin, 1973). Receiver operating characteristic (ROC) curve analysis (OriginPro 2016, OriginLab Corporation, Northampton, USA) was used to determine the optimal cut-off values (safety margin thresholds) between the three different cholestasis classes and to evaluate the accuracy by which cholestasis classes can be separated. ROC analysis calculates the sensitivity (fraction of true positive (TP) classifications) and specificity (fraction of true negative (TN) classifications) for any possible cut-off value and plots sensitivity against 1- specificity representing the ROC curve. The optimal cut-off values correspond to the maximum rate of correct positive and negative classifications and were determined by minimizing the distance (d) between point [0,1] in the ROC space (where sensitivity and specificity are maximum) and any point on the ROC curve (Kumar and Indrayan, 2011):

$$d^2 = (1 - TP)^2 + (1 - TN)^2 \quad (12)$$

The separation of cholestasis classes by the estimated safety margin thresholds was compared using the area under the ROC curves (ROC AUCs), were 1.0 represents a perfect discrimination between two classes and 0.5 represents the poorest discrimination.

Quantification of physiological and genetic factors. A theoretical assessment for the impact of disease state and polymorphic pathways on DIC was conducted using bosentan as example drug compound. The impact of disease state on $C_{sys,u}$ concentrations was estimated based on literature observations that pulmonary arterial hypertension (PAH) patients show 2-fold increased systemic bosentan concentrations compared to healthy volunteers

DMD Fast Forward. Published on March 2, 2017 as DOI: 10.1124/dmd.116.074179
This article has not been copyedited and formatted. The final version may differ from this version.

(Dingemanse and van Giersbergen, 2004). The resulting hepatic inlet and intrahepatic concentrations were calculated according to eq. 8 and 10 using a $C_{sys,u}$ value of 0.1327 µM.

The effect of nonsynonymous polymorphisms of hepatic metabolic enzymes and transporters on the *in vitro* Kp_{uu} of bosentan was calculated according to eq. 13 using measured *in vitro* process clearances (Table 1), their fractional *in vivo* contributions (fn) and reported fold changes in activity compared to the reference genotype (α):

$$Kp_{uu} = \frac{\alpha_{OATP1B1} \times fn_{OATP1B1} \times PS_{inf,act} + \alpha_{OATP1B3} \times fn_{OATP1B3} \times PS_{inf,act} + PS_{inf,pas}}{PS_{eff} + \alpha_{CYP3A4} \times fn_{CYP3A4} \times CL_{int,met} + \alpha_{CYP2C9} \times fn_{CYP2C9} \times CL_{int,met} + \alpha_{MRP2} \times fn_{MRP2} \times CL_{int,sec}} \quad (13)$$

The α values used were determined from the following data: Increased activity was reported for the organic anion transporting polypeptide (OATP) variants OATP1B1*1b and OATP1B3*2 ($\alpha_{OATP1B1} = \alpha_{OATP1B3} = 2$) (Rowland and Matin, 1973; Letschert et al., 2004). The cytochrome P450 (CYP) variants CYP3A4*20 and CYP2C9*3 are associated with loss-of function ($\alpha_{CYP3A4} = \alpha_{CYP2C9} = 0$) (Lee et al., 2002; Werk and Cascorbi, 2014), similar to the multidrug resistance protein (MRP) 2 variant MRP2*16 (c.2302C>T) ($\alpha_{MRP2} = 0$) (Hulot et al., 2005; Pratt et al., 2015). According to the literature OATP1B1 and OATP1B3 equally contribute to the total active hepatic uptake of bosentan ($fn_{OATP1B1} = fn_{OATP1B3} = 0.5$) (Treiber et al., 2007). Hepatic metabolism is mediated by CYP3A4 ($fn_{CYP3A4} = 0.6$) and CYP2C9 ($fn_{CYP2C9} = 0.4$) (Dingemanse and van Giersbergen, 2004), and biliary secretion is mediated by MRP2 ($fn_{MRP2} = 1.0$) (Fahrmayr et al., 2013).

To estimate the potential impact of BSEP polymorphisms on the DIC safety margin, reduced BSEP activity was assumed to mimic an increased inhibition potential, where 100% activity corresponds to the BSEP IC_{50} value of bosentan (22 µM). According to the literature, BSEP G855R (c.2563G>A) has < 20% transport activity compared to non-polymorphic BSEP (Lang et al., 2007), which was simulated using a 5-fold reduced BSEP IC_{50} value (4.4 µM).

DMD Fast Forward. Published on March 2, 2017 as DOI: 10.1124/dmd.116.074179
This article has not been copyedited and formatted. The final version may differ from this version.

Results

Kp_{uu} and ECM class assignment. *In vitro* measured hepatic process clearances for the 18 investigated drug compounds are summarized in Table 1 together with the resulting *in vitro* Kp_{uu} values, which range from 0.07 to 2.41. Fig. 3 displays the corresponding fold-change in intracellular unbound drug concentrations ($C_{hep,u}$) calculated from extracellular concentrations and *in vitro* Kp_{uu}, where atazanavir and pravastatin represent the extremes with ~14-fold decreased and ~2.4-fold increased $C_{hep,u}$, respectively.

Compound classification according to ECM is based on the extent of individual hepatic *in vitro* clearance processes (Fig. 2). As hepatic clearance processes significantly impact intrahepatic concentrations as illustrated in Fig. 2 and Fig. 3, ECM class-dependent effects on Kp_{uu} values can be expected. For the ECM class 1 compound ketoconazole, a Kp_{uu} value < 1 was obtained as a result of a predominant intrinsic clearance contribution (i.e. PS_{eff} + CL_{int} > PS_{inf}). On the other hand, for ECM class 2 compounds imatinib and verapamil Kp_{uu} was mainly determined by passive uptake and efflux processes and consequently approached values of 1 (i.e. PS_{eff} + CL_{int} ≈ PS_{inf}). For the ECM class 3 compounds with predominant intrinsic clearance (atazanavir, erythromycin, ibuprofen, lovastatin acid, rosiglitazone and simvastatin acid) Kp_{uu} values < 1 were obtained (i.e. PS_{eff} + CL_{int} > PS_{inf}). The ECM class 3 compounds with substantial active hepatic uptake, namely atorvastatin and cyclosporine A, exhibit Kp_{uu} values > 1 (i.e. PS_{eff} + CL_{int} < PS_{inf}). Similarly, the ECM class 4 compounds bosentan, cerivastatin, fluvastatin, glibenclamide, pitavastatin, pravastatin and rosuvastatin reveal Kp_{uu} values > 1 due to predominant hepatic uptake (i.e. PS_{eff} + CL_{int} < PS_{inf}).

***In vitro-in vivo* correlation of Kp_{uu} in rat.** Estimation of $C_{hep,u}$ using ECM-based *in vitro* Kp_{uu} data implies that the *in vitro* Kp_{uu} directly translates to *in vivo* Kp_{uu}. We made this assumption based on previous successful applications of the ECM approach for hepatic clearance and DDI predictions (Camenisch and Umehara, 2012; Umehara and Camenisch, 2012; Kunze et al., 2015). To further validate the ECM concept, we performed an IVIVC for Kp_{uu} in rat using published in-house data (Umehara and Camenisch, 2012) (Fig. 4). In addition, IVIVC of

DMD Fast Forward. Published on March 2, 2017 as DOI: 10.1124/dmd.116.074179
This article has not been copyedited and formatted. The final version may differ from this version.

reported *in vitro* Kp_{uu} values from initial rate hepatic uptake clearances in suspended hepatocytes (Yabe et al., 2011; Shitara et al., 2013) and from sandwich-cultured hepatocytes (Pfeifer et al., 2013) are shown in Fig. 4. Observed (*in vivo*) and predicted (*in vitro*) Kp_{uu} data following the ECM concept were in good agreement with all five compounds deviating by less than 2.5-fold. Also Kp_{uu} from rat sandwich-cultured hepatocytes demonstrated close IVIVC for three compounds. In contrast, *in vitro* Kp_{uu} from suspended hepatocytes generally provided overestimations of *in vivo* Kp_{uu}, most likely due to the absence of intrinsic clearance processes (metabolism and biliary secretion).

For atorvastatin, cyclosporine A and verapamil, different ECM classes were assigned for rat and human, due to different contributions of the individual clearance processes. The impact of *in vitro* and *in vivo* Kp_{uu} values in rat, however, was in line with the ECM theory described above (ECM class 1: $Kp_{uu} < 1$; ECM class 4: Kp_{uu} values > 1).

Correlation between BSEP inhibition, drug concentrations and drug induced cholestasis. The assignment of the 18 test drug compounds into the three cholestasis frequency classes (“no”, “rare”, “common”) is shown in Table 2. Risk assessments with regard to DIC were conducted using safety margins calculated as the ratio of BSEP IC_{50} and either unbound extracellular drug concentrations ($C_{sys,u}$ or $C_{inlet,u}$) or unbound intracellular concentrations upon application of Kp_{uu} ($C_{hep,sys,u}$ or $C_{hep,inlet,u}$) (Fig. 5). The risk assessment with unbound systemic concentrations showed a separation between drugs in cholestasis classes ”common” and ”no cholestasis” while drugs in the class ”rare” markedly overlapped with drugs in the other classes (Fig. 5A). The separation of drugs in cholestasis class ”rare” from “common” or ”no cholestasis” was not improved by using the substantially higher unbound drug concentrations at the hepatic inlet (Fig. 5B). This incomplete separation of the cholestasis classes based on extracellular concentrations is reflected by ROC AUC values of 0.83 - 0.94. In contrast, the use of unbound intrahepatic drug concentrations following Kp_{uu} correction markedly enhanced the separation between the three cholestasis classes. The risk assessment based on $C_{hep,sys,u}$ provided a good separation between the three classes with only one drug (rosiglitazone, class “no”) being clearly mispredicted (Fig. 5C). The risk

DMD Fast Forward. Published on March 2, 2017 as DOI: 10.1124/dmd.116.074179
This article has not been copyedited and formatted. The final version may differ from this version.

assessment was further improved by using Kp_{uu}-corrected unbound hepatic inlet concentrations. Using this reference concentration an almost complete separation of all drugs into classes “no”, ”rare” and ”common” was achieved (Fig. 5D), as supported by ROC AUC values of ≥ 0.97. Using $C_{hep,inlet,u}$ as a reference, safety margin thresholds between classes “common”/”rare” and “rare”/”no” of 26 and 529 were obtained, respectively (Fig. 5D). These thresholds are clearly lower than those obtained from risk assessments using unbound extracellular concentrations (Fig. 5A and 5B; “common”/”rare”: 100 and 59, “rare”/”no”: 3821 and 728 for $C_{sys,u}$ and $C_{inlet,u}$, respectively). Using $C_{hep,inlet,u}$ the safety margin of simvastatin was reduced to 584-fold compared to 69667-fold based on $C_{hep,sys,u}$, representing the largest safety margin change within our test set.

Additionally, maximum (“worst-case”) unbound hepatic inlet concentrations ($C_{inlet,max,u}$) were calculated in order to represent the situation during early drug development where no clinical data are available. Assuming fast and complete intestinal absorption, substantially higher unbound intrahepatic concentrations were obtained than using measured clinical parameters. While the resulting ratios still allowed to separate ”common” from “rare” cholestasis events, the separation between “no” and “rare” was poorer than that obtained in risk assessments based on measured clinical parameters (Fig. 5D vs 5E).

Quantification of risk factors for DIC. The theoretical impact of disease state and polymorphic hepatic enzymes and transporters on bosentan-induced cholestasis was estimated based on clinical systemic exposure and *in vitro* enzyme and transporter polymorphism data (Fig. 6). The systemic exposure of bosentan is reported to be ~2-fold higher in PAH patients compared to healthy subjects (Dingemanse and van Giersbergen, 2004). Based on this, we calculated the corresponding $C_{hep,inlet,u}$ in PAH patients (0.1901 µM), which is 69% higher than in healthy subjects (Fig. 6, “healthy” vs “PAH patients”). Next, we calculated Kp_{uu}, $C_{hep,inlet,u}$ and corresponding safety margins for bosentan using altered transporter and enzyme activities due to genetic polymorphisms according to eq. 13. Our assessment indicates that the increased transport activity of OATP1B1*1b or OATP1B3*2 variants would increase Kp_{uu} and $C_{hep,inlet,u}$ by 17% (Fig. 6, “PAH patients” vs “OATP1B1*1b”

DMD Fast Forward. Published on March 2, 2017 as DOI: 10.1124/dmd.116.074179
This article has not been copyedited and formatted. The final version may differ from this version.

or “OATP1B3*2”). Loss-of-function mutations in CYP3A4, CYP2C9 and MRP2 would result in increases in both Kp_{uu} and $C_{hep,inlet,u}$ by 14%, 9% and 1%, respectively (Fig. 6, “PAH patients” vs “CYP3A4*20” or “CYP2C9*3” or “MRP2*16”). Assuming concurrence of all these genetic variants leads to predicted increases of Kp_{uu} and $C_{hep,inlet,u}$ by 70% and a reduction of the safety margin from 116 to 68 (Fig. 6, “PAH patients” vs “CYP3A4*20, CYP2C9*3, MRP2*16, OATP1B1*1b, OATP1B3*2”). Additionally, we evaluated the potential impact of BSEP polymorphisms on the DIC risk assessment. Presence of the low activity variant BSEP G885R was simulated using a 5-fold reduced BSEP IC_{50} value (4.4 µM). This estimation leads to a 23-fold safety margin (Fig. 6, “PAH patients” vs “BSEP G885R”). The theoretical combination of the BSEP G885R variant with genetic variants that affect the Kp_{uu} of bosentan would even further increase the DIC risk as shown in Fig. 6 (“PAH patients” vs “BSEP G885R, CYP3A4*20, CYP2C9*3, MRP2*16, OATP1B1*1b, OATP1B3*2”).

DMD Fast Forward. Published on March 2, 2017 as DOI: 10.1124/dmd.116.074179
This article has not been copyedited and formatted. The final version may differ from this version.

Discussion

In the present work we compare the use of unbound extracellular (systemic and hepatic inlet) or Kp_{uu}–based intrahepatic concentrations in risk assessments of cholestasis upon BSEP inhibition.

Our work follows up on recent studies, which investigated the impact of systemic drug exposure on the clinical manifestation of DIC or DILI. Using safety margin ratios of BSEP IC_{50} to systemic drug concentration, our analyses revealed a generally increased risk of DIC among drugs with lower safety margins (Fig. 5A). However, no reliable separation of cholestatic and non-cholestatic drugs was obtained from this assessment. The outcome was not improved when hepatic inlet concentrations were used for safety margin calculations (Fig. 5B), even though this concentration is considered as most relevant with regards to inhibition of hepatic enzymes or transporters (Zamek-Gliszczynski et al., 2013). These observations based on extracellular concentrations are in line with the previous studies using similar approaches (Dawson et al., 2012; Morgan et al., 2013; Shah et al., 2015). However, several differences to previous work are important to highlight: 1) Following the “free drug hypothesis” we used only unbound drug concentrations rather than total drug concentrations. Indeed, we obtained poorer predictions of DIC using total drug concentrations in plasma or blood (data not shown); 2) We evaluated the association of BSEP inhibition with DIC only and not with other types of liver toxicity. Hepatocellular DILI cases, which are included in other studies, are rather caused by direct toxicity or immune-mediated reactions (Chen et al., 2015) and are likely not explained by BSEP inhibition; 3) We classified the investigated drugs according to the DIC incidence instead of a commonly used DILI severity grading (Chen et al., 2011; Pedersen et al., 2013; Aleo et al., 2014); 4) The present assessment represents a “worst-case” scenario using the lowest reported *in vitro* BSEP IC_{50} (variability in IC_{50} values was within a 3-fold range for the majority of dugs with exception of cyclosporine A, erythromycin, glibenclamide and rosiglitazone) and the maximum reported systemic drug concentration at steady-state after administration of the highest recommended oral dose. At least for certain drugs (e.g. $C_{sys,u}$ of atorvastatin and rosiglitazone), our parameters

significantly deviate from previous studies (Dawson et al., 2012; Morgan et al., 2013; Shah et al., 2015).

However, relating extracellular drug concentrations to inhibition of an intracellular liver target (BSEP) is not expected to provide meaningful risk estimations if intracellular drug concentrations are affected by active transport or metabolic processes (Dawson et al., 2012; Chu et al., 2013; Camenisch et al., 2015; Camenisch, 2016). Indeed, applying the *in vitro* Kp_{uu} values to obtain unbound intrahepatic drug concentrations markedly improved the separation of cholestasis classes. This became particularly evident for the correlation with unbound intrahepatic concentrations based on hepatic inlet concentrations, where almost complete separation between the different cholestasis classes was obtained (Fig. 5D). The use of hepatic inlet concentrations is most important for drugs with high hepatic first-pass elimination and significantly reduced systemic concentrations, as observed for simvastatin (115-fold difference between $C_{sys,u}$ and $C_{inlet,u}$). We therefore conclude that the unbound intrahepatic drug concentration based on hepatic inlet concentrations clearly represents the most reliable reference concentration for prediction of the DIC risk using BSEP inhibition assays.

BSEP *in vitro* inhibition data are commonly generated in early drug development. However, at this stage clinical drug exposure data are rarely available and DIC risk assessments based on the presented approach are not possible. We therefore performed an alternative risk assessment assuming that the clinical systemic exposure can accurately be predicted and assuming complete and rapid absorption to obtain “worst-case” hepatic inlet concentrations (Fig. 5E) (Ito et al., 1998; Giacomini et al., 2010). While the cholestasis classes “common” and “rare” were reasonably-well separated by this approach, the separation between classes “no cholestasis” and “rare” failed compared to risk approaches using measured clinical input parameters (Fig. 5D vs Fig. 5E). For DIC risk assessments during preclinical development, we therefore suggest to apply unbound intrahepatic drug concentrations derived from *in vitro* Kp_{uu} and predicted systemic exposure (e.g. using PBPK modeling).

DMD Fast Forward. Published on March 2, 2017 as DOI: 10.1124/dmd.116.074179
This article has not been copyedited and formatted. The final version may differ from this version.

Kp_{uu} and corresponding unbound intrahepatic drug concentrations are affected by the individual contributions of active hepatic transport and metabolic processes and correlate well with the four ECM classes (Fig. 2, Fig. 3). For drugs in ECM classes 1 and 3, where hepatic uptake is the rate-limiting elimination step, Kp_{uu} is likely to be below 1 ($C_{hep,u} < C_u$). On the other hand, class 3 drugs can also approach Kp_{uu} above 1 if active hepatic uptake is extensive ($C_{hep,u} > C_u$). As illustrated in Fig. 7, unbound extracellular concentrations of ketoconazole and simvastatin acid markedly overestimated the DIC risk. Use of Kp_{uu}-corrected unbound intrahepatic concentrations shifted ketoconazole (Kp_{uu} = 0.32) and simvastatin acid (Kp_{uu} = 0.39) into their appropriate risk zones (“rare” and “no” cholestasis, respectively). For class 4 drugs, passive uptake/efflux permeability exceeds intrinsic hepatic clearance. In combination with active hepatic uptake processes, drugs accumulate within the hepatocytes resulting in Kp_{uu} values greater 1 (Fig. 2, Fig. 3). For these drugs the DIC risk is underestimated by unbound extracellular concentrations as highlighted for pitavastatin in Fig. 7. After correction with Kp_{uu} pitavastatin was assigned to the correct risk zone (“rare”). Only for class 2 drugs such as imatinib do unbound extracellular concentrations represent an appropriate surrogate for the unbound intrahepatic concentration ($Kp_{uu} \approx 1.0$, $C_{hep,u} \approx C_u$) (Fig. 7).

For the *in vitro* Kp_{uu} assessment we generally assumed absence of active sinusoidal efflux. Kp_{uu} values of substrates for basolateral MRP3 and MRP4, which have been shown to be upregulated in human and rat under cholestatic conditions (Soroka et al., 2001; Gradhand et al., 2008), might therefore be over-predicted. However, except for rosuvastatin, the relevance of MRP3 and MRP4 in transport of pharmaceutical drugs is unknown and requires further research. In addition, we assumed that the ECM-based *in vitro* Kp_{uu} directly translates to *in vivo* Kp_{uu}. The assumption was based on the good IVIVC for Kp_{uu} in rat (Fig. 4) and on previous hepatic clearance predictions using the ECM, where no systematic under-prediction of *in vivo* hepatic clearance was observed. Similarly, *in vitro* Kp_{uu} using sandwich-cultured hepatocytes recently provided a close IVIVC in rat for rosuvastatin, ritonavir and furamidine (Pfeifer et al., 2013), whereas Kp_{uu} from suspended hepatocytes generally over-predicted

DMD Fast Forward. Published on March 2, 2017 as DOI: 10.1124/dmd.116.074179
This article has not been copyedited and formatted. The final version may differ from this version.

Kp_{uu} *in vivo*, likely due to the absence of intrinsic clearance processes. Partial loss of activity in certain *in vitro* systems has previously been described (Lundquist et al., 2014), however, the need of scaling factors for PK modeling is controversially discussed and likely compound-dependent requiring clinical data (Jones et al., 2012; Morse et al., 2015; Yoshikado et al., 2016). Especially in an early drug development stage the direct use of *in vitro* Kp_{uu} is therefore expected to enable estimations of unbound intrahepatic drug concentrations.

Our risk assessment using unbound hepatic inlet concentrations predicted a DIC risk in more than 2% of subjects for safety margins below ~25 (Fig. 5D). Since unbound intracellular concentrations are 25-fold below the IC_{50} of BSEP, no relevant inhibition of BSEP would be expected. However, the occurrence of DIC in few percent of patients leads us to the hypothesis that these subjects react more sensitively to BSEP inhibition than the rest of the population. This variability might be explained by various physiological (e.g. age, gender, underlying diseases), exogenous (e.g. co-medication, nutrition) and genetic factors (polymorphisms) that potentially modify intrahepatic drug concentrations or BSEP activity, resulting in increased cholestasis risk. Using bosentan as an example we evaluated the theoretical impact of disease state and polymorphic hepatic enzymes and transporters on the DIC risk (Fig. 6). Physiological factors such as increased age and gender are not associated with altered risk of bosentan-induced cholestasis (Markova et al., 2013). Similarly, increased systemic bosentan exposure in PAH patients could not be linked to higher incidence of liver injury (Dingemanse and van Giersbergen, 2004), which is in line with our assessment (Fig. 6). The present analysis suggests that genetic variants of transporters and enzymes involved in bosentan elimination only marginally affect the DIC risk assessment, even upon the unlikely concurrence of all polymorphisms (Fig. 6). Indeed, bosentan-induced liver injury could not be associated with polymorphic variants of OATP1B1, OATP1B3, CYP2C9 or MRP2 (Markova et al., 2013; Markova et al., 2014; Roustit et al., 2014). In addition, we evaluated the impact of the BSEP variant G885R, which was recently associated with DIC, likely due to substantially reduced activity (< 20%) (Lang et al., 2007). Based on this data, we estimated a significantly increased risk of bosentan-induced cholestasis in PAH patients

carrying the G885R variant as indicated by a 23-fold safety margin and the change in cholestasis class from “rare” to “common” (Fig. 6). In summary, the presented risk assessment for bosentan illustrates the utility of ECM-based Kp_{uu} assessments in order to define the relevance of polymorphic enzymes and transporters in the hepatic elimination of a drug. Especially for drugs with high risk of DIC such information could guide the selection of genotyping targets in clinics and ultimately allow providing personalized dosing regimens. However, further research on frequency, global distribution and *in vivo* effects of polymorphisms will be required to estimate the incidence of DIC in heterogenic populations.

In conclusion, we demonstrated that the incidence of DIC upon BSEP inhibition correlates with Kp_{uu}-based unbound intrahepatic drug concentrations. To the best of our knowledge, this approach represents the most reliable prediction of DIC available so far, which in addition allows to account for polymorphisms on hepatic enzymes and transporters associated with DIC risk. Our study represents a proof-of-concept for estimating the inhibition potential of an intracellular transporter and is therefore expected to likewise improve risk assessments for other intrahepatic targets involved in DDI, pharmacologic efficacy and toxicology such as hyperbilirubinemia upon MRP2 or UGT1A1 inhibition. The validation of ECM-based risk assessments for other target enzymes or transporter as well as the extension of the approach to other organs such as the kidney will require extensive future research.

DMD Fast Forward. Published on March 2, 2017 as DOI: 10.1124/dmd.116.074179
This article has not been copyedited and formatted. The final version may differ from this version.

Acknowledgements

The authors thank the many Novartis Drug Metabolism and Pharmacokinetics scientists of Basel, Switzerland, who have supported this work. Special thank goes to Marc Witschi, Judith Streckfuss and Hans-Joachim Handschin for technical assistance, to Kenichi Umehara and Ewa Gatlik for scientific advice and to David Pearson for critical evaluation of this manuscript.

DMD Fast Forward. Published on March 2, 2017 as DOI: 10.1124/dmd.116.074179
This article has not been copyedited and formatted. The final version may differ from this version.

Autorship Contributions

Participated in research design: Riede, Poller, and Camenisch

Conducted experiments: Riede

Performed data analysis: Riede, Poller, and Camenisch

Wrote or contributed to the writing of the manuscript: Riede, Poller, Huwyler, and Camenisch

References

Aleo MD, Luo Y, Swiss R, Bonin PD, Potter DM, and Will Y (2014) Human drug-induced liver injury severity is highly associated with dual inhibition of liver mitochondrial function and bile salt export pump. *Hepatology* **60:**1015-1022.

Bjornsson E and Olsson R (2005) Outcome and prognostic markers in severe drug-induced liver disease. *Hepatology* **42:**481-489.

Camenisch G, Riede J, Kunze A, Huwyler J, Poller B, and Umehara K (2015) The extended clearance model and its use for the interpretation of hepatobiliary elimination data. *ADMET & DMPK* **3:**1-14.

Camenisch G and Umehara K (2012) Predicting human hepatic clearance from in vitro drug metabolism and transport data: a scientific and pharmaceutical perspective for assessing drug-drug interactions. *Biopharmaceutics & drug disposition* **33:**179-194.

Camenisch GP (2016) Drug Disposition Classification Systems in Discovery and Development: A Comparative Review of the BDDCS, ECCS and ECCCS Concepts. *Pharmaceutical research* **33:**2583-2593.

Chen M, Suzuki A, Borlak J, Andrade RJ, and Lucena MI (2015) Drug-induced liver injury: Interactions between drug properties and host factors. *J Hepatol* **63:**503-514.

Chen M, Vijay V, Shi Q, Liu Z, Fang H, and Tong W (2011) FDA-approved drug labeling for the study of drug-induced liver injury. *Drug Discov Today* **16:**697-703.

Chu X, Korzekwa K, Elsby R, Fenner K, Galetin A, Lai Y, Matsson P, Moss A, Nagar S, Rosania GR, Bai JP, Polli JW, Sugiyama Y, Brouwer KL, and International Transporter C (2013) Intracellular drug concentrations and transporters: measurement, modeling, and implications for the liver. *Clin Pharmacol Ther* **94:**126-141.

CIOMS (1999) *Reporting Adverse Drug Reactions - Definitions of Terms and Criteria for their Use*, Geneva.

Dawson S, Stahl S, Paul N, Barber J, and Kenna JG (2012) In vitro inhibition of the bile salt export pump correlates with risk of cholestatic drug-induced liver injury in humans. *Drug metabolism and disposition: the biological fate of chemicals* **40:**130-138.

Dietrich CG and Geier A (2014) Effect of drug transporter pharmacogenetics on cholestasis. *Expert opinion on drug metabolism & toxicology* **10:**1533-1551.

Dingemanse J and van Giersbergen PL (2004) Clinical pharmacology of bosentan, a dual endothelin receptor antagonist. *Clin Pharmacokinet* **43:**1089-1115.

Fahrmayr C, Konig J, Auge D, Mieth M, Munch K, Segrestaa J, Pfeifer T, Treiber A, and Fromm M (2013) Phase I and II metabolism and MRP2-mediated export of bosentan in a MDCKII-OATP1B1-CYP3A4-UGT1A1-MRP2 quadruple-transfected cell line. *Br J Pharmacol* **169:**21-33.

Fattinger K, Funk C, Pantze M, Weber C, Reichen J, Stieger B, and Meier PJ (2001) The endothelin antagonist bosentan inhibits the canalicular bile salt export pump: a potential mechanism for hepatic adverse reactions. *Clin Pharmacol Ther* **69:**223-231.

FDA (2009) Guidance for Industry. Drug-Induced Liver Injury: Premarketing Clinical Evaluation.

Funk C, Pantze M, Jehle L, Ponelle C, Scheuermann G, Lazendic M, and Gasser R (2001) Troglitazone-induced intrahepatic cholestasis by an interference with the hepatobiliary export of bile acids in male and female rats. Correlation with the gender difference in troglitazone sulfate formation and the inhibition of the canalicular bile salt export pump (Bsep) by troglitazone and troglitazone sulfate. *Toxicology* **167:**83-98.

Giacomini KM, Huang SM, Tweedie DJ, Benet LZ, Brouwer KL, Chu X, Dahlin A, Evers R, Fischer V, Hillgren KM, Hoffmaster KA, Ishikawa T, Keppler D, Kim RB, Lee CA, Niemi M, Polli JW, Sugiyama Y, Swaan PW, Ware JA, Wright SH, Yee SW, Zamek-Gliszczynski MJ, and Zhang L (2010) Membrane transporters in drug development. *Nat Rev Drug Discov* **9:**215-236.

Gradhand U, Lang T, Schaeffeler E, Glaeser H, Tegude H, Klein K, Fritz P, Jedlitschky G, Kroemer HK, Bachmakov I, Anwald B, Kerb R, Zanger UM, Eichelbaum M, Schwab M, and Fromm MF (2008) Variability in human hepatic MRP4 expression: influence of cholestasis and genotype. *Pharmacogenomics J* **8:**42-52.

Hulot JS, Villard E, Maguy A, Morel V, Mir L, Tostivint I, William-Faltaos D, Fernandez C, Hatem S, Deray G, Komajda M, Leblond V, and Lechat P (2005) A mutation in the drug transporter gene ABCC2 associated with impaired methotrexate elimination. *Pharmacogenet Genomics* **15:**277-285.

Hussaini SH and Farrington EA (2007) Idiosyncratic drug-induced liver injury: an overview. *Expert Opin Drug Saf* **6:**673-684.

Ito K, Iwatsubo T, Kanamitsu S, Ueda K, Suzuki H, and Sugiyama Y (1998) Prediction of pharmacokinetic alterations caused by drug-drug interactions: metabolic interaction in the liver. *Pharmacol Rev* **50:**387-412.

Jones HM, Barton HA, Lai Y, Bi YA, Kimoto E, Kempshall S, Tate SC, El-Kattan A, Houston JB, Galetin A, and Fenner KS (2012) Mechanistic pharmacokinetic modeling for the prediction of transporter-mediated disposition in humans from sandwich culture human hepatocyte data. *Drug metabolism and disposition: the biological fate of chemicals* **40:**1007-1017.

Kumar R and Indrayan A (2011) Receiver operating characteristic (ROC) curve for medical researchers. *Indian Pediatr* **48:**277-287.

Kunze A, Huwyler J, Camenisch G, and Poller B (2014) Prediction of organic anion-transporting polypeptide 1B1- and 1B3-mediated hepatic uptake of statins based on transporter protein expression and activity data. *Drug metabolism and disposition: the biological fate of chemicals* **42:**1514-1521.

Kunze A, Poller B, Huwyler J, and Camenisch G (2015) Application of the extended clearance concept classification system (ECCCS) to predict the victim drug-drug interaction potential of statins. *Drug Metab Pers Ther* **30:**175-188.

Kwon Y (2001) *Handbook of Essential Pharmacokinetics, Pharmacodynamics, and Drug Metabolism for Industrial Scientists*. Kluwer Academic/Plenum Publishers, New York.

Lang C, Meier Y, Stieger B, Beuers U, Lang T, Kerb R, Kullak-Ublick GA, Meier PJ, and Pauli-Magnus C (2007) Mutations and polymorphisms in the bile salt export pump and the

multidrug resistance protein 3 associated with drug-induced liver injury. *Pharmacogenet Genomics* **17:**47-60.

Lee CR, Goldstein JA, and Pieper JA (2002) Cytochrome P450 2C9 polymorphisms: a comprehensive review of the in-vitro and human data. *Pharmacogenetics* **12:**251-263.

Lee WM (2003) Drug-induced hepatotoxicity. *N Engl J Med* **349:**474-485.

Letschert K, Keppler D, and Konig J (2004) Mutations in the SLCO1B3 gene affecting the substrate specificity of the hepatocellular uptake transporter OATP1B3 (OATP8). *Pharmacogenetics* **14:**441-452.

Lundquist P, Loof J, Sohlenius-Sternbeck AK, Floby E, Johansson J, Bylund J, Hoogstraate J, Afzelius L, and Andersson TB (2014) The impact of solute carrier (SLC) drug uptake transporter loss in human and rat cryopreserved hepatocytes on clearance predictions. *Drug metabolism and disposition: the biological fate of chemicals* **42:**469-480.

Markova SM, De Marco T, Bendjilali N, Kobashigawa EA, Mefford J, Sodhi J, Le H, Zhang C, Halladay J, Rettie AE, Khojasteh C, McGlothlin D, Wu AH, Hsueh WC, Witte JS, Schwartz JB, and Kroetz DL (2013) Association of CYP2C9*2 with bosentan-induced liver injury. *Clin Pharmacol Ther* **94:**678-686.

Markova SM, Schwartz JB, and Kroetz DL (2014) Response to "CYP2C9 polymorphism is not a major determinant of bosentan exposure in healthy volunteers". *Clin Pharmacol Ther* **95:**252.

Mateus A, Matsson P, and Artursson P (2013) Rapid measurement of intracellular unbound drug concentrations. *Mol Pharm* **10:**2467-2478.

Morgan RE, van Staden CJ, Chen Y, Kalyanaraman N, Kalanzi J, Dunn RT, 2nd, Afshari CA, and Hamadeh HK (2013) A multifactorial approach to hepatobiliary transporter assessment enables improved therapeutic compound development. *Toxicological sciences : an official journal of the Society of Toxicology* **136:**216-241.

Morse BL, Cai H, MacGuire JG, Fox M, Zhang L, Zhang Y, Gu X, Shen H, Dierks EA, Su H, Luk CE, Marathe P, Shu YZ, Humphreys WG, and Lai Y (2015) Rosuvastatin Liver Partitioning in Cynomolgus Monkeys: Measurement In Vivo and Prediction Using In Vitro

Monkey Hepatocyte Uptake. *Drug metabolism and disposition: the biological fate of chemicals* **43:**1788-1794.

Muller PY and Milton MN (2012) The determination and interpretation of the therapeutic index in drug development. *Nat Rev Drug Discov* **11:**751-761.

Nicolai J, De Bruyn T, Van Veldhoven PP, Keemink J, Augustijns P, and Annaert P (2015) Verapamil hepatic clearance in four preclinical rat models: towards activity-based scaling. *Biopharmaceutics & drug disposition* **36:**462-480.

Olson H, Betton G, Robinson D, Thomas K, Monro A, Kolaja G, Lilly P, Sanders J, Sipes G, Bracken W, Dorato M, Van Deun K, Smith P, Berger B, and Heller A (2000) Concordance of the toxicity of pharmaceuticals in humans and in animals. *Regul Toxicol Pharmacol* **32:**56-67.

Pauli-Magnus C, Meier PJ, and Stieger B (2010) Genetic determinants of drug-induced cholestasis and intrahepatic cholestasis of pregnancy. *Semin Liver Dis* **30:**147-159.

Pedersen JM, Matsson P, Bergstrom CA, Hoogstraate J, Noren A, LeCluyse EL, and Artursson P (2013) Early identification of clinically relevant drug interactions with the human bile salt export pump (BSEP/ABCB11). *Toxicological sciences : an official journal of the Society of Toxicology* **136:**328-343.

Pfeifer ND, Harris KB, Yan GZ, and Brouwer KL (2013) Determination of intracellular unbound concentrations and subcellular localization of drugs in rat sandwich-cultured hepatocytes compared with liver tissue. *Drug metabolism and disposition: the biological fate of chemicals* **41:**1949-1956.

Pratt VM, Beyer BN, Koller DL, Skaar TC, Flockhart DA, Levy KD, and Vance GH (2015) Report of new haplotype for ABCC2 gene: rs17222723 and rs8187718 in cis. *J Mol Diagn* **17:**201-205.

Roustit M, Fonrose X, Montani D, Girerd B, Stanke-Labesque F, Gonnet N, Humbert M, and Cracowski JL (2014) CYP2C9, SLCO1B1, SLCO1B3, and ABCB11 polymorphisms in patients with bosentan-induced liver toxicity. *Clin Pharmacol Ther* **95:**583-585.

Rowland M and Matin SB (1973) Kinetics of Drug-Drug Interactions. *Journal of pharmacokinetics and biopharmaceutics* **1:**553-567.

Shah F, Leung L, Barton HA, Will Y, Rodrigues AD, Greene N, and Aleo MD (2015) Setting Clinical Exposure Levels of Concern for Drug-Induced Liver Injury (DILI) Using Mechanistic in vitro Assays. *Toxicological sciences : an official journal of the Society of Toxicology* **147:**500-514.

Shitara Y, Maeda K, Ikejiri K, Yoshida K, Horie T, and Sugiyama Y (2013) Clinical significance of organic anion transporting polypeptides (OATPs) in drug disposition: their roles in hepatic clearance and intestinal absorption. *Biopharmaceutics & drug disposition* **34:**45-78.

Soroka CJ, Lee JM, Azzaroli F, and Boyer JL (2001) Cellular localization and up-regulation of multidrug resistance-associated protein 3 in hepatocytes and cholangiocytes during obstructive cholestasis in rat liver. *Hepatology* **33:**783-791.

Stieger B (2010) Role of the bile salt export pump, BSEP, in acquired forms of cholestasis. *Drug Metab Rev* **42:**437-445.

Stieger B, Fattinger K, Madon J, Kullak-Ublick GA, and Meier PJ (2000) Drug- and estrogen-induced cholestasis through inhibition of the hepatocellular bile salt export pump (Bsep) of rat liver. *Gastroenterology* **118:**422-430.

Treiber A, Schneiter R, Hausler S, and Stieger B (2007) Bosentan is a substrate of human OATP1B1 and OATP1B3: inhibition of hepatic uptake as the common mechanism of its interactions with cyclosporin A, rifampicin, and sildenafil. *Drug metabolism and disposition: the biological fate of chemicals* **35:**1400-1407.

Umehara K and Camenisch G (2012) Novel in vitro-in vivo extrapolation (IVIVE) method to predict hepatic organ clearance in rat. *Pharmaceutical research* **29:**603-617.

Werk AN and Cascorbi I (2014) Functional gene variants of CYP3A4. *Clin Pharmacol Ther* **96:**340-348.

Yabe Y, Galetin A, and Houston JB (2011) Kinetic characterization of rat hepatic uptake of 16 actively transported drugs. *Drug metabolism and disposition: the biological fate of chemicals* **39:**1808-1814.

Yoshikado T, Yoshida K, Kotani N, Nakada T, Asaumi R, Toshimoto K, Maeda K, Kusuhara H, and Sugiyama Y (2016) Quantitative Analyses of Hepatic OATP-Mediated Interactions Between Statins and Inhibitors Using PBPK Modeling With a Parameter Optimization Method. *Clin Pharmacol Ther* **100:**513-523.

Zamek-Gliszczynski MJ, Lee CA, Poirier A, Bentz J, Chu X, Ellens H, Ishikawa T, Jamei M, Kalvass JC, Nagar S, Pang KS, Korzekwa K, Swaan PW, Taub ME, Zhao P, and Galetin A (2013) ITC recommendations for transporter kinetic parameter estimation and translational modeling of transport-mediated PK and DDIs in humans. *Clin Pharmacol Ther* **94:**64-79.

DMD Fast Forward. Published on March 2, 2017 as DOI: 10.1124/dmd.116.074179
This article has not been copyedited and formatted. The final version may differ from this version.

Figure Legends

FIG. 1. Extended Clearance Model (ECM) and Kp_{uu}. Schematic diagram of hepatic clearance processes determining the liver-to-blood partition coefficient for unbound drug at steady-state (Kp_{uu}). The unbound intrahepatic concentration ($C_{hep,u}$) is determined by the unbound extracellular concentration (C_u) and the interplay between all hepatic process clearances, where $C_{hep,u} = C_u \times Kp_{uu}$. Unbound drug in the blood stream, is taken up into hepatocytes (PS_{inf}) by transporters ($PS_{inf,act}$) and/or by passive diffusion ($PS_{inf,pas}$). Elimination of drug from the hepatocyte (CL_{int}) occurs via hepatic metabolism ($CL_{int,met}$), by active secretion into bile ($CL_{int,sec}$) and by sinusoidal efflux (PS_{eff}) via active transport ($PS_{eff,act}$) and/or passive diffusion ($PS_{eff,pas}$).

FIG. 2. Drug classification according to ECM and expected impact on Kp_{uu} and $C_{hep,u}$. ECM class 1/2 was assigned if $PS_{eff} < CL_{int}$, otherwise class 3/4. Class 1/3 was assigned if $PS_{eff} = PS_{inf}$, otherwise class 2/4. In the present study, PS_{eff} was assumed to occur only via passive diffusion and to be equal to $PS_{inf,pas}$ ($PS_{eff} = PS_{inf,pas}$). Adapted from Camenisch et al. (2015).

FIG. 3. ECM class-dependent impact of experimentally determined hepatic process clearances on $K_{p,uu}$ and $C_{hep,u}$. The black lines represent the x-fold change of intrahepatic concentrations ($C_{hep,u}$) depending on Kp_{uu}. X-fold increase and decrease in $C_{hep,u}$ corresponds to Kp_{uu} and $1/Kp_{uu}$, respectively. White, grey and dark grey bars represent the underlying process clearances (active uptake, sum of passive uptake and efflux, and intrinsic clearance, respectively), which affect Kp_{uu}, as described in Fig. 2. Hepatic process clearances refer to the left y-axis whereas changes in $C_{hep,u}$ refer to the right y-axis.

FIG. 4. *In vitro-in vivo* correlation of hepatic Kp_{uu} in rat. Rat *in vitro* Kp_{uu} values were calculated according to ECM (eqs. 1 and 3) using published in-house *in vitro* hepatic process clearance data or were taken from the literature. Rat *in vivo* Kp_{uu} values were derived from reported liver partition and drug binding data. Detailed calculations of Kp_{uu} and literature references are summarized in Supplemental Table 1. Black diamonds refer to ECM-based Kp_{uu} (in-house data), white squares, triangles and circles represent *in vitro* Kp_{uu} obtained by

DMD Fast Forward. Published on March 2, 2017 as DOI: 10.1124/dmd.116.074179
This article has not been copyedited and formatted. The final version may differ from this version.

Pfeifer et al. (2013), Yabe et al. (2011) and Shitara et al. (2013), respectively. The solid line is the line of unity. Numbers represent the investigated drugs: 1. atorvastatin, 2. cyclosporine A, 3. furamidine, 4. ketoconazole, 5. pravastatin, 6. ritonavir, 7. rosuvastatin, 8. verapamil.

FIG. 5. Correlation between BSEP inhibition, drug concentration and drug-induced cholestasis. Safety margins for all 18 drug compounds representing the ratio of BSEP IC_{50} value and A, unbound systemic concentration ($C_{sys,u}$). B, unbound concentration at the hepatic inlet ($C_{inlet,u}$). C, unbound intrahepatic concentration on basis of $C_{sys,u}$ ($C_{hep,sys,u}$). D, unbound intrahepatic concentration on basis of $C_{inlet,u}$ ($C_{hep,inlet,u}$). E, "worst-case" assessment of maximum unbound intrahepatic concentration ($C_{hep,inlet,max,u}$). Red, yellow and green symbols represent the cholestasis classes "common", "rare" and "no cholestasis", respectively. Squares, circles, triangles and diamonds represent the ECM classes 1, 2, 3, and 4, respectively. Estimated safety margin thresholds between the cholestasis classes "common"/ "rare" and " rare"/ "no cholestasis" are shown next to dashed lines with ROC AUCs in brackets.

FIG. 6. Theoretical impact of polymorphic hepatic enzymes and transporters on DIC safety margins for bosentan. $C_{hep,inlet,u}$ of bosentan (125 mg bid) in PAH patients in various enzyme/transporter polymorphism scenarios was calculated from extracellular $C_{inlet,u}$ and *in vitro* Kp_{uu} using *in vitro* activity data (eq. 13). Contributions of transporters and CYP enzymes to the hepatic bosentan clearance as well as functional impact of polymorphisms are described in materials and methods section. The dashed line represents the safety margin threshold between the cholestasis classes "common"/ "rare" (26-fold).

FIG. 7. ECM class dependent effect of Kp_{uu} on the DIC risk assessment. BSEP IC_{50} values were plotted against unbound hepatic inlet concentrations before ($C_{inlet,u}$) and after correction with *in vitro* Kp_{uu} to unbound intrahepatic concentrations ($C_{hep,inlet,u}$). Ketoconazole (class 1), imatinib (class 2), simvastatin acid (class 3) and pitavastatin are shown as yellow squares, red circles, green triangles and yellow diamonds, respectively. Red, yellow and green symbols represent the cholestasis classes "common", "rare" and "no cholestasis",

DMD Fast Forward. Published on March 2, 2017 as DOI: 10.1124/dmd.116.074179
This article has not been copyedited and formatted. The final version may differ from this version.

respectively. Dashed lines represent the safety margin thresholds between cholestasis classes ”common”/ ”rare” (26-fold) and ”rare”/ ”no” (529-fold), respectively.

Tables

TABLE 1: *In vitro* process clearances, *in vitro* Kp_{uu} and human drug exposure.

Drug compounds	Hepatic process clearances				*in vitro*	Unbound extracellular concentrations		Unbound intrahepatic concentrations		BSEP inhibition
	$PS_{inf,act}$	$PS_{inf,pas}$ [a)]	$CL_{int,met}$	$CL_{int,sec}$	Kp_{uu}	$C_{sys,u}$	$C_{inlet,u}$	$C_{hep,sys,u}$	$C_{hep,inlet,u}$	IC_{50}
	[ml/min/kg]					[µM]				
ECM class 1										
Ketoconazole	0.0	58.5	97.4	29.6	0.32	0.1661	0.2941	0.0532	0.0941	2.9
ECM class 2										
Imatinib	0.0	300.9	40.9	3.2	0.87	0.4781	1.1534	0.4159	1.0035	< 10
Verapamil	0.0	258.2	127.7	8.1	0.66	0.0607	0.2398	0.0401	0.1583	20.5
ECM class 3										
Atazanavir	71.8	20.8	1240.5	41.0	0.07	1.1653	2.3500	0.0816	0.1645	3.1
Atorvastatin	140.3	57.7	64.6	11.1	1.48	0.0226	0.0819	0.0334	0.1212	15.0
Cyclosporine A	113.2	41.9	77.6	9.1	1.21	0.0512	0.1371	0.0620	0.1659	0.4
Erythromycin	10.2	20.3	99.7	8.9	0.24	1.0083	1.1334	0.2420	0.2720	4.1
Ibuprofen	22.2	21.7	34.2	10.3	0.66	3.9289	5.1880	2.5931	3.4241	598.6

Lovastatin acid	165.1	145.5	459.0	0	0.51	0.0050	0.0114	0.0026	0.0058	19.3
Rosiglitazone	45.6	46.6	98.1	0	0.64	0.0036	0.0048	0.0023	0.0031	1.9
Simvastatin acid	116.1	297.9	769.2	1.5	0.39	0.0008	0.0917	0.0003	0.0358	20.9
ECM class 4										
Bosentan(125 mg bid)	30.7	61.5	16.2	0.8	1.17	0.0663	0.0960	0.0776	0.1123	22.0
Bosentan (1000 mg bid)	30.7	61.5	16.2	0.8	1.17	0.4644	0.9312	0.5433	1.0895	22.0
Cerivastatin	221.5	243.8	46.9	0	1.60	0.0003	0.0005	0.0005	0.0008	18.8
Fluvastatin	218.7	325.5	146.8	0	1.15	0.0052	0.0133	0.0060	0.0153	36.1
Glibenclamide	66.4	109.6	41.1	6.3	1.12	0.0094	0.0133	0.0105	0.0149	1.5
Pitavastatin	364.3	258.8	17.7	0	2.25	0.0111	0.0392	0.0245	0.0882	42.2
Pravastatin	578.0	36.0	0.9	2.1	2.41	0.0716	0.7999	0.1726	1.9278	268.4
Rosuvastatin	27.2	24.8	1.5	5.8	1.62	0.0092	0.0670	0.0149	0.1085	197.6

ECM classes were derived as described in Fig. 2. Unbound extracellular (systemic and hepatic inlet) and intracellular concentrations were calculated as described in “Materials and Methods” and all required pharmacokinetic parameters and corresponding literature references are summarized in Supplemental Tables 2 - 4. Literature references for BSEP IC_{50} values are provided in Supplemental Table 5, presented data represent the lowest available IC_{50} value. [a)] In the present study, PS_{eff} was assumed to occur only via passive diffusion and to be equal to $PS_{inf,pas}$ ($PS_{eff} = PS_{inf,pas}$). bid = twice daily.

DMD Fast Forward. Published on March 2, 2017 as DOI: 10.1124/dmd.116.074179
This article has not been copyedited and formatted. The final version may differ from this version.

TABLE 2: Cholestasis classification.

Cholestasis class	Drug compounds
common (> 2%)	bosentan (1000 mg bid), cyclosporine A, erythromycin, imatinib
rare (≤ 2%)	atazanavir, atorvastatin, bosentan (125 mg bid), glibenclamide, ibuprofen, ketoconazole, pitavastatin, pravastatin, verapamil
no cholestasis	cerivastatin, fluvastatin, lovastatin acid, rosiglitazone, rosuvastatin, simvastatin acid

Bosentan was assigned to the classes “common” and “rare” depending on the administered dose (1000 and 125 mg twice daily (bid), respectively). Literature references and detailed annotations are summarized in Supplemental Table 5.

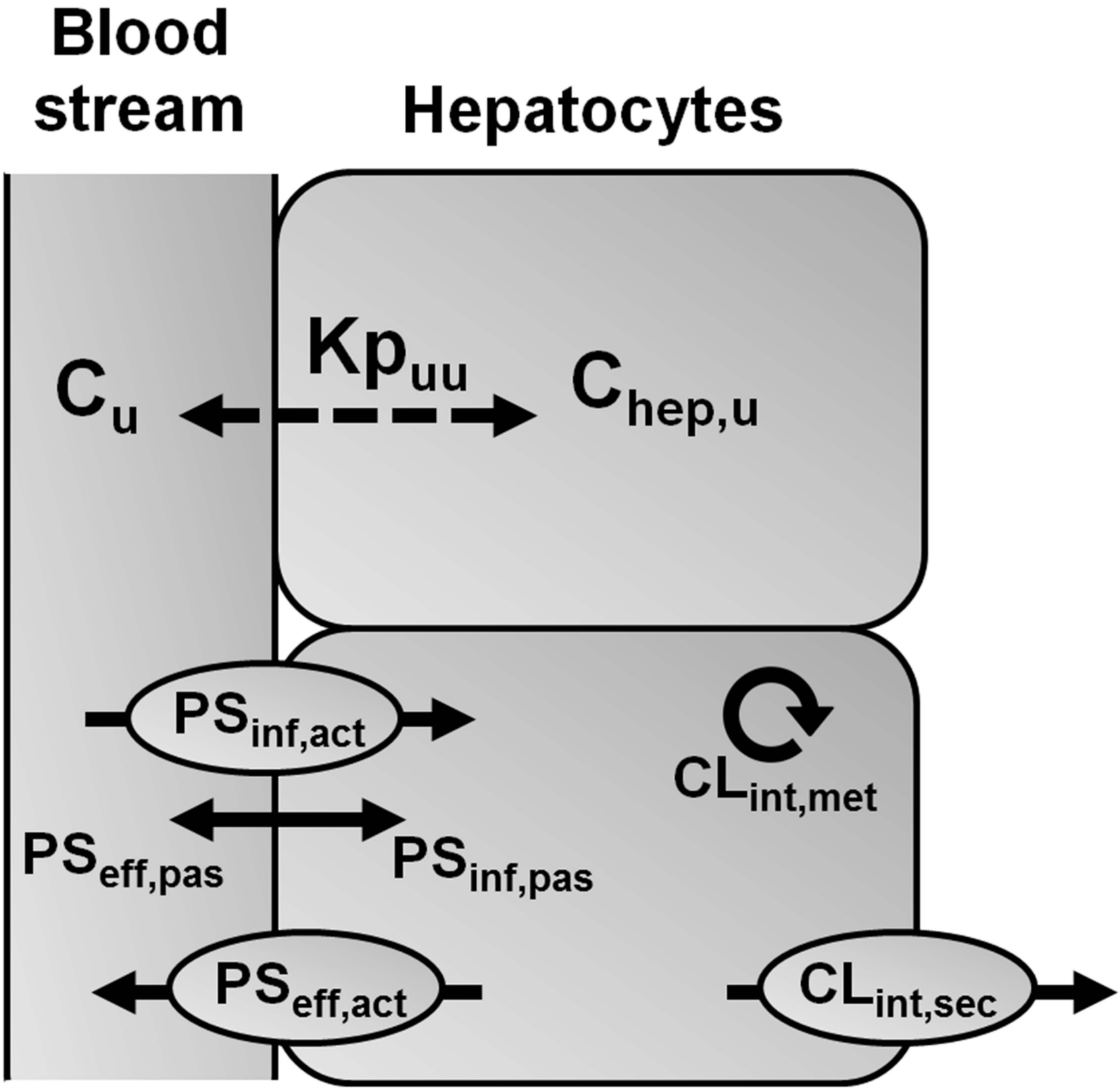
Blood stream
Hepatocytes
C_u
Kp_{uu}
$C_{hep,u}$
$PS_{inf,act}$
$CL_{int,met}$
$PS_{eff,pas}$
$PS_{inf,pas}$
$PS_{eff,act}$
$CL_{int,sec}$

Figure 1

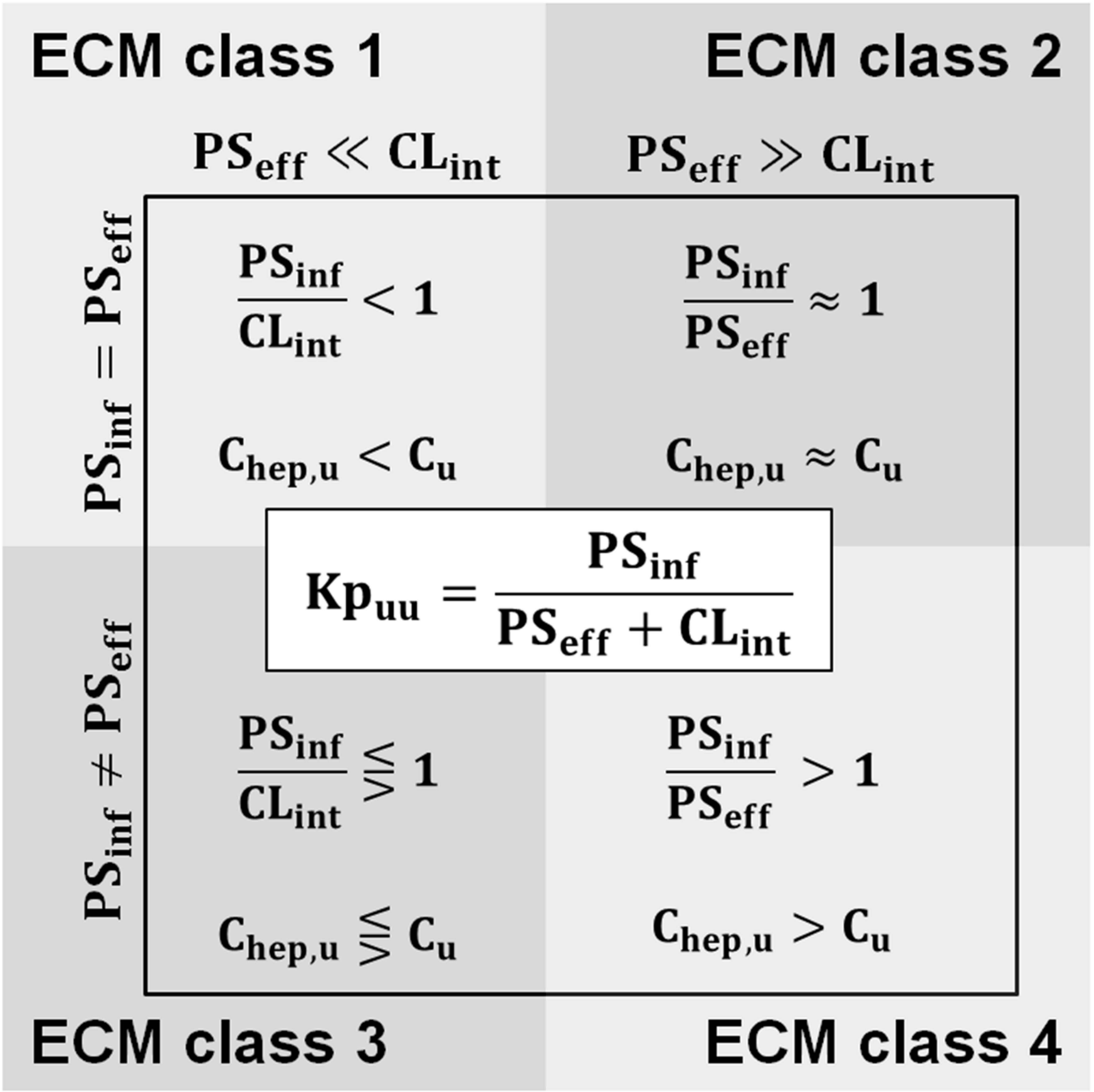
ECM class 1
ECM class 2
$PS_{eff} \ll CL_{int}$
$PS_{eff} \gg CL_{int}$
$PS_{inf} = PS_{eff}$
$\frac{PS_{inf}}{CL_{int}} < 1$
$\frac{PS_{inf}}{PS_{eff}} \approx 1$
$C_{hep,u} < C_u$
$C_{hep,u} \approx C_u$
$Kp_{uu} = \frac{PS_{inf}}{PS_{eff} + CL_{int}}$
$PS_{inf} \neq PS_{eff}$
$\frac{PS_{inf}}{CL_{int}} \lessgtr 1$
$\frac{PS_{inf}}{PS_{eff}} > 1$
$C_{hep,u} \lessgtr C_u$
$C_{hep,u} > C_u$
ECM class 3
ECM class 4

Figure 2

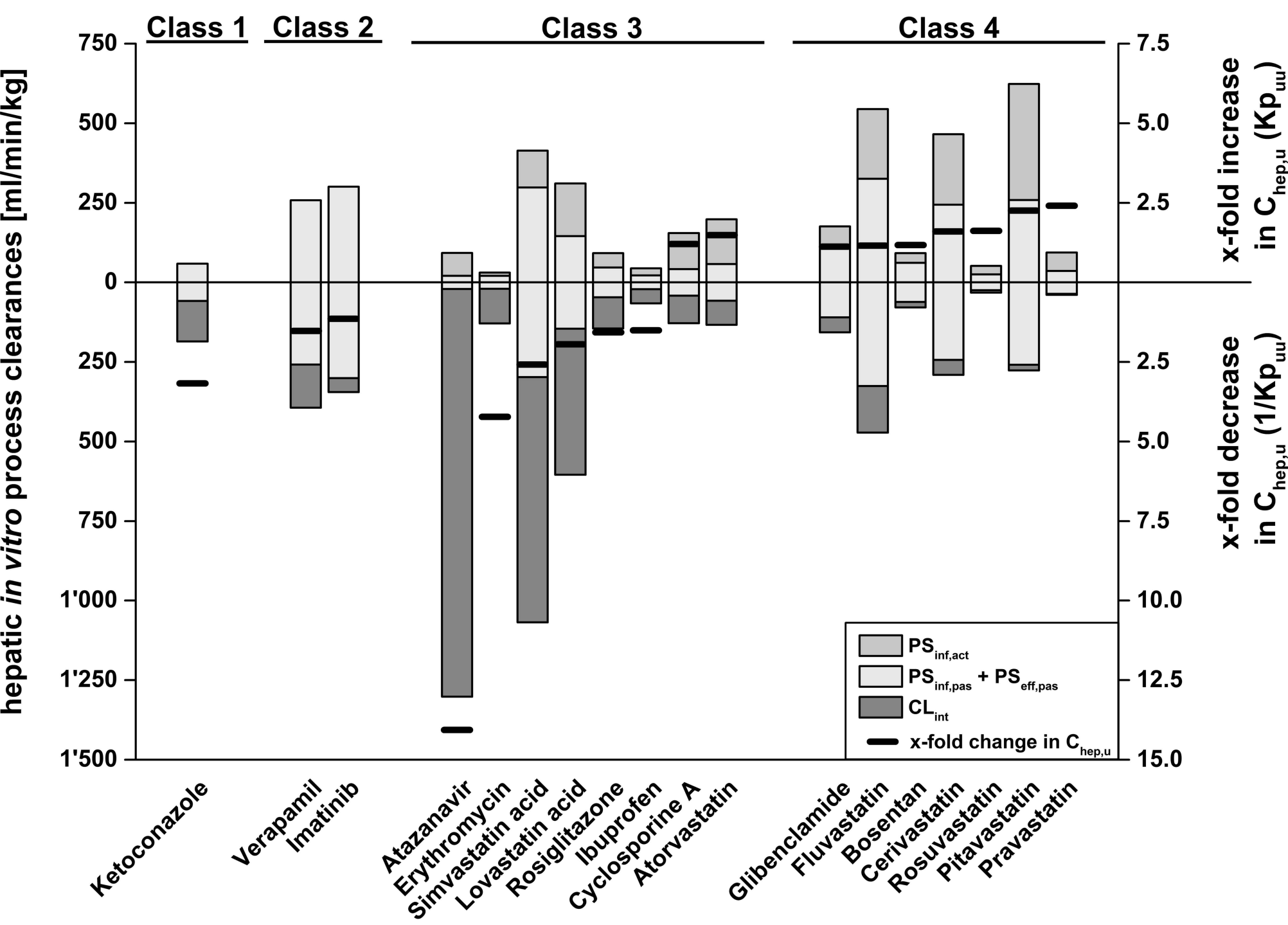
Class 1
Class 2
Class 3
Class 4
hepatic in vitro process clearances [ml/min/kg]
750
500
250
0
250
500
750
1'000
1'250
1'500
7.5
5.0
2.5
2.5
5.0
7.5
10.0
12.5
15.0
x-fold increase in $C_{hep,u}$ (Kp_{uu})
x-fold decrease in $C_{hep,u}$ ($1/Kp_{uu}$)
$PS_{inf,act}$
$PS_{inf,pas}$ + $PS_{eff,pas}$
CL_{int}
x-fold change in $C_{hep,u}$
Ketoconazole
Verapamil
Imatinib
Atazanavir
Erythromycin
Simvastatin acid
Lovastatin acid
Rosiglitazone
Ibuprofen
Cyclosporine A
Atorvastatin
Glibenclamide
Fluvastatin
Bosentan
Cerivastatin
Rosuvastatin
Pitavastatin
Pravastatin

Figure 3

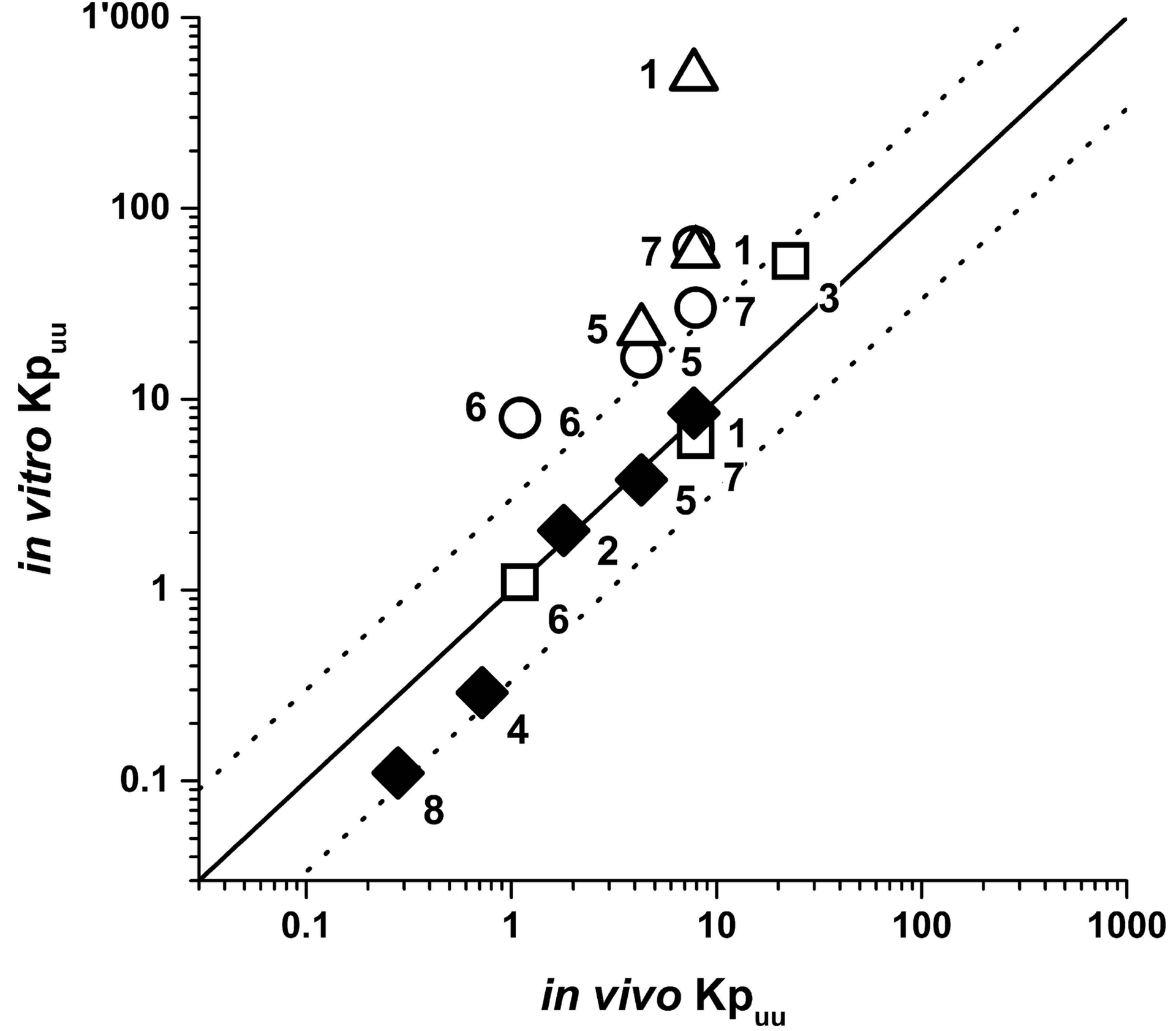
1'000
100
10
1
0.1
in vitro Kp$_{uu}$
0.1
1
10
100
1000
in vivo Kp$_{uu}$
1
7
1
7
3
5
5
6
6
1
7
5
2
6
4
8

Figure 4

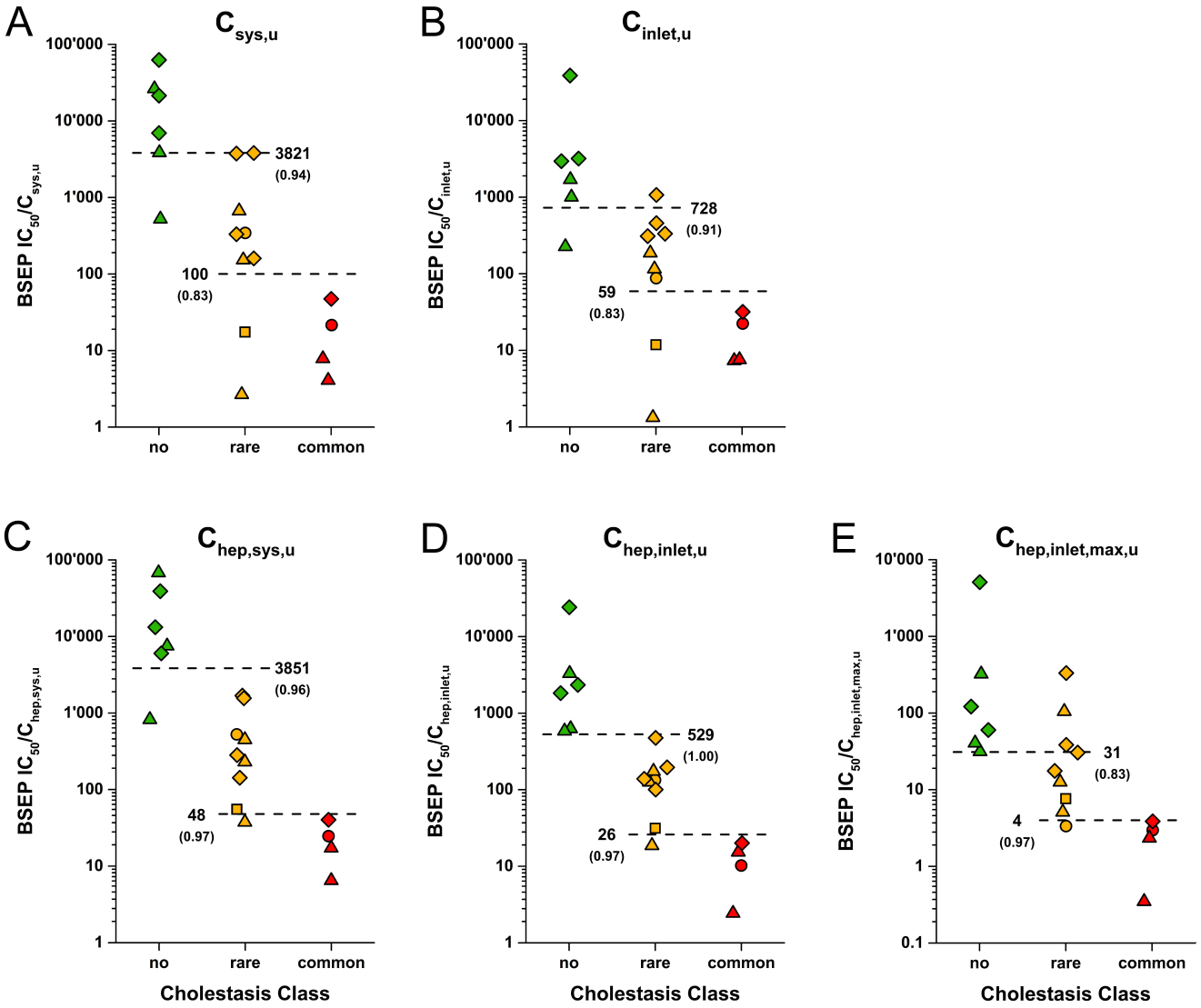
A
$c_{sys,u}$
BSEP $IC_{50}/C_{sys,u}$
100'000
10'000
1'000
100
10
1
3821
(0.94)
100
(0.83)
no
rare
common
B
$c_{inlet,u}$
BSEP $IC_{50}/C_{inlet,u}$
728
(0.91)
59
(0.83)
C
$c_{hep,sys,u}$
BSEP $IC_{50}/C_{hep,sys,u}$
3851
(0.96)
48
(0.97)
Cholestasis Class
D
$c_{hep,inlet,u}$
BSEP $IC_{50}/C_{hep,inlet,u}$
529
(1.00)
26
(0.97)
E
$c_{hep,inlet,max,u}$
BSEP $IC_{50}/C_{hep,inlet,max,u}$
0.1
31
(0.83)
4
(0.97)

Figure 5

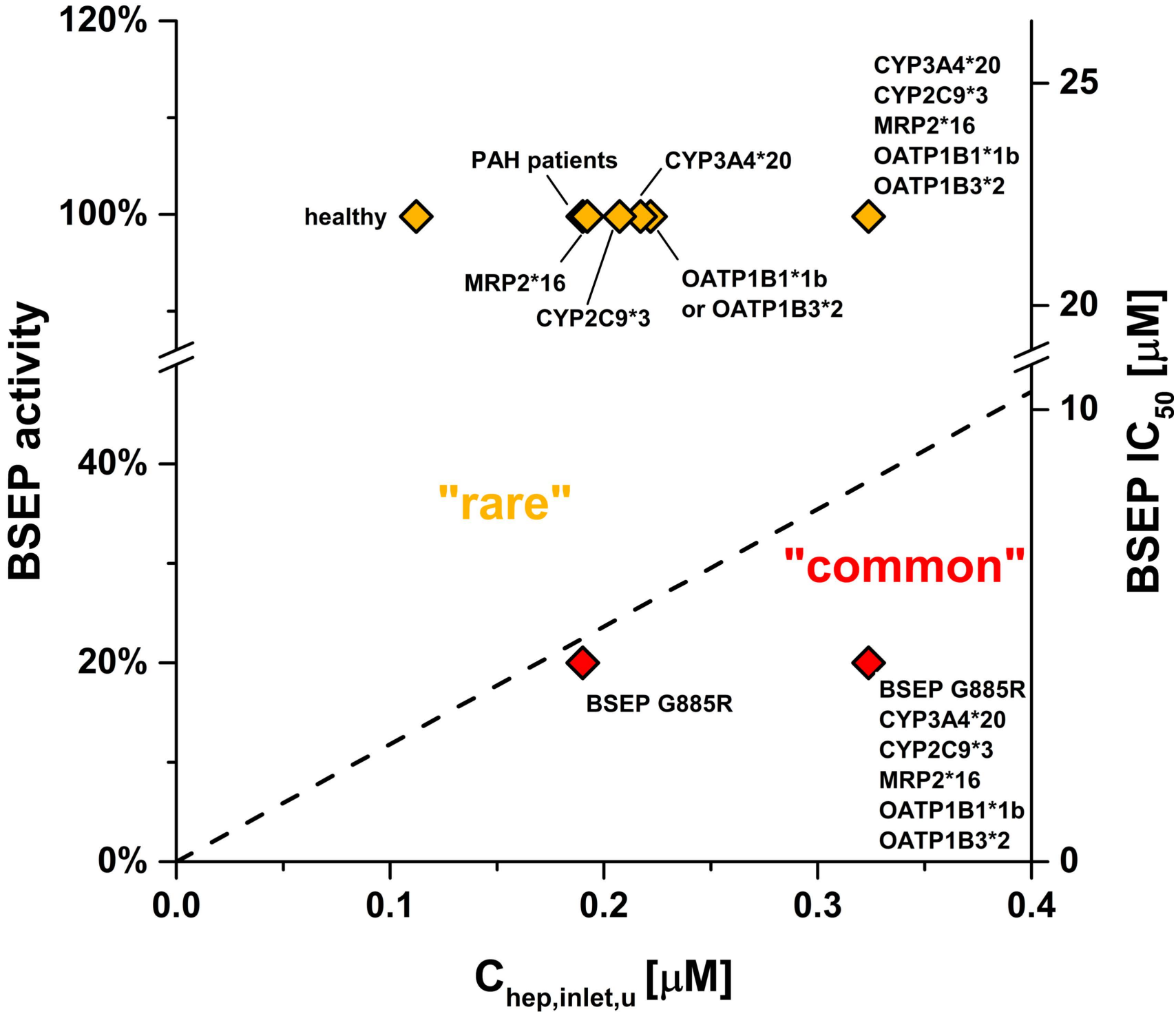
120%
100%
40%
20%
0%
BSEP activity
25
20
10
0
BSEP IC50 [µM]
0.0
0.1
0.2
0.3
0.4
Chep,inlet,u [µM]
healthy
PAH patients
CYP3A4*20
MRP2*16
CYP2C9*3
OATP1B1*1b
or OATP1B3*2
CYP3A4*20
CYP2C9*3
MRP2*16
OATP1B1*1b
OATP1B3*2
"rare"
"common"
BSEP G885R
BSEP G885R
CYP3A4*20
CYP2C9*3
MRP2*16
OATP1B1*1b
OATP1B3*2

Figure 6

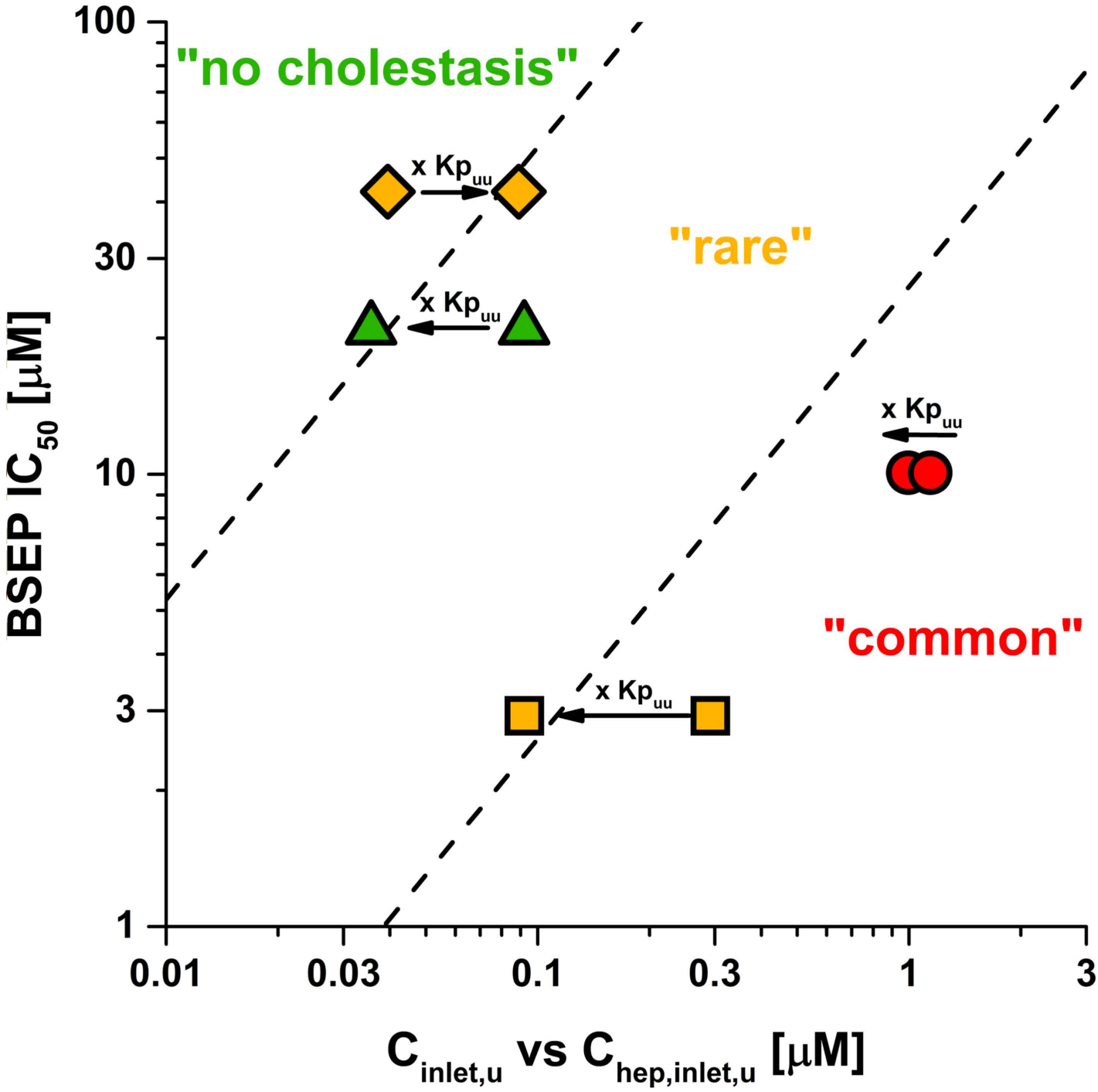
"no cholestasis"
"rare"
"common"
x Kp$_{uu}$
x Kp$_{uu}$
x Kp$_{uu}$
x Kp$_{uu}$
BSEP IC$_{50}$ [µM]
100
30
10
3
1
0.01
0.03
0.1
0.3
1
3
C$_{inlet,u}$ vs C$_{hep,inlet,u}$ [µM]

Figure 7